Accurate and Efficient Unions of Balls

Nina Amenta and Ravi Krishna Kolluri[†]
University of Texas at Austin

Abstract

Given a sample of points from the boundary of an object in $\mathbb{R}^3$, we construct a representation of the object as a union of balls. We use many fewer balls than previous constructions, but our shape representation is better. We bound the distance from the surface of the union to the original object surface, and show that when the sampling is sufficiently dense the two are homeomorphic. This implies a topological relationship between the true medial axis of the object and both the medial axis, and the α-shape, of the union of balls. We show that the set of ball centers in our construction converges to the true medial axis as the sampling density increases.

1 Introduction

Any object can be represented as a union of balls: the *Medial Axis Transform* represents an object $\mathcal{W}$ as the union of the (generally infinite) set of maximal balls contained in its interior. It is often convenient, in $\mathbb{R}^3$, to approximate this representation with a finite set $\mathcal{B}$ of balls such that $\bigcup \mathcal{B}$ resembles $\mathcal{W}$. Generally $\mathcal{B}$ is found by taking the Voronoi diagram of a dense set S of point samples on the boundary W of $\mathcal{W}$, finding the set P_V of Voronoi vertices in the interior of $\mathcal{W}$, and using the set $\mathcal{B}_V$ of all Voronoi balls with centers in P_V. We point out that a subset of these Voronoi vertices, the set P_I of *interior poles*, actually gives a better approximation of $\mathcal{W}$. Under the assumption that S is a sufficiently dense sample from W, we prove that the boundary of the union of the set B_I of Voronoi balls centered at points of P_I is close to W, that its surface normals are close to nearby normals on W, and that it is homeomorphic W.

The portion of the Voronoi diagram of S interior to $\mathcal{W}$ has been used as a discrete approximation of the *medial axis* of $\mathcal{W}$; the centers of $\mathcal{B}_V$ form the vertices of this approximation. In three dimensions $\mathcal{B}_V$ contains many balls with centers close to the object surface, corresponding to flat "sliver" tetrahedra in the Delaunay triangulation of S, as shown in Figure 1. These balls may be (and almost always are) present even when the data is completely noise-free, at any finite sampling density. Their centers form the endpoints of long branches (or "hairs") on the approximate medial axis, which have no relation to any actual feature of $\mathcal{W}$, and must be removed with a heuristic clean-up step. Using $\mathcal{B}_I$, rather than $\mathcal{B}_V$, leads immediately to easily

[†] Computer Sciences Dept., Austin, TX 78712, USA. Supported by NSF/CCR-9731977. rkolluri@cs.utexas.edu

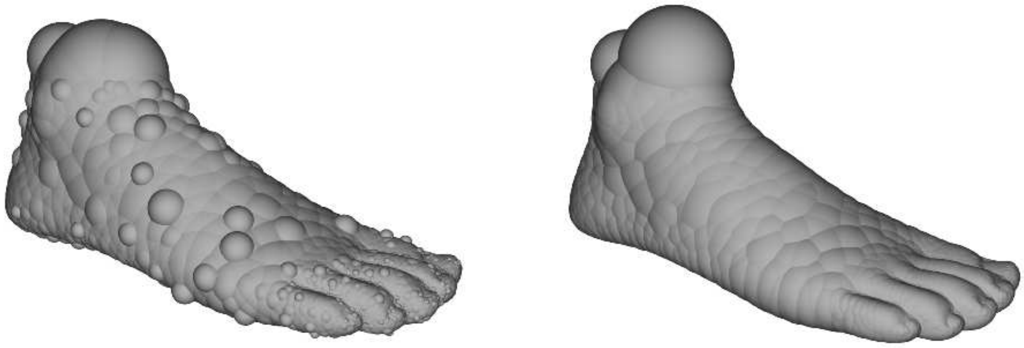

Figure 1: Left, the usual construction: the union of all 10,093 interior Voronoi balls. Right, the union of the 2,931 interior *polar balls*. The "warts" on the first model are due not to noise, but to discretization, and would appear at any finite sampling density.

computable, and better, approximations to the three-dimensional medial axis (see Figure 2). One is the weighted α-shape, or *dual shape* as defined by Edelsbrunner [6]. A second is the medial axis of the union of the B_I, which, as Attalli and Montanvert [2] have shown, is easily computable in this special case. We prove that both of these

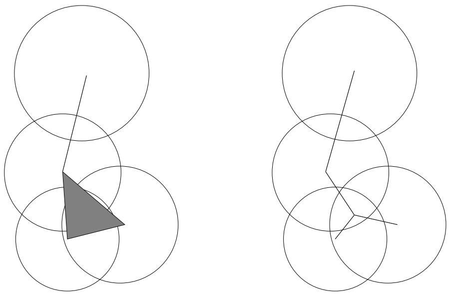

Figure 2: Left, the dual shape of a union of balls, and their medial axis, right.

constructions are homotopy equivalent to the medial axis of W, and that the set P_I of inner poles, which belongs to both, converges to the medial axis of W as the sampling density increases. This is not true of P_V.

Finding P_I is actually easier than finding P_V. To find P_V, an inside/outside test must be performed for each Voronoi vertex, typically by intersecting an infinite ray starting at the vertex with the model. The interior poles, on the other hand, are easy to identify with local operations using the Voronoi diagram itself.

2 Motivation and related work

Our main motivation for studying $\mathcal{B}_I$ is that we plan to use it as a tool for polygonal surface reconstruction. But finite unions of balls and discrete medial axis transforms have many other applications as well.

Hubbard [8] promotes the use of unions of balls for collision detection, guided by the observation that detecting the intersection of two balls is much easier than detecting intersections of two other primitives like triangles or polyhedra. He constructs a hierarchical representation, using increasingly simple unions of balls, and gives convincing experimental evidence that this hierarchy is more efficient in practice than others. Hubbard's experience shows that the success of the approach depends on the quality of the shape approximation. He finds that $\mathcal{B}_V$ is superior to a larger and less accurate set of balls derived from a quadtree; we believe that $\mathcal{B}_I$ should be better still.

Finite unions of balls or discrete medial axis transforms have also been proposed as a representation for deformable objects. Rajan and Fournier [9] use a union of balls for interpolating between shapes. Teichman and Teller [11] use a discrete medial axis as a skeleton in a semi-automatic system for animating arbitrary computer models. Both papers again begin with $\mathcal{B}_V$ and use a heuristic clean-up phase, and again, we believe that $\mathcal{B}_I$ would be a better starting point. Cheng, Edelsbrunner, Fu and Lam [3] do morphing in two dimensions with *skin surfaces*, which are smooth surfaces based on unions of balls. Our work can be seen as a step toward converting an arbitrary polygonal surface into a provably accurate skin surface.

The computation of the exact medial axis for simple polyhedra has been demonstrated only recently [5]. For more complicated shapes, approximation probably continues to be more appropriate. Attalli and Montanvert [2] and others [10] have proposed approximating the medial axis using the Voronoi diagram. This approach is sometimes justified by a reference to [7], which argues, incorrectly, that P_V converges to the true medial axis as the sampling density increases. Since P_I *does* converge to the medial axis, we believe that the discrete approximations based on P_I should be much better.

3 Union of interior poles

We let S be a sample from a smooth object surface W. For simplicity, we will that S is contained in a large bounding box, so that all Voronoi vertices of samples in S are finite. We use the notation $B_{c,\rho}$ for the ball of radius ρ centered at c.

Definition: The *poles* of a sample s are the two vertices of its Voronoi cell farthest from s, one on either side of the surface. When c is a pole of some sample s, the Voronoi ball $B_{c,\rho}$ is a *polar ball*, with $\rho = d(c, s)$.

Amenta and Bern [1] show that both poles of s are found correctly by the following procedure: select the Voronoi vertex of s farthest from s as the first pole p_1. From among those Voronoi vertices v of s such that the angle $\angle vsp_1 > \pi/2$, select the farthest as the second pole. The orientation of the surface W determines which is the inside, and which the outside pole.

The intuition behind this paper is that the polar balls approximate medial balls. Let P be the set of poles. The surface W divides the set of poles into the set P_I of *inside poles* and the set P_O of *outside poles.*

Definition: Let $\mathcal{U}_I$ be the union of Voronoi balls centered at inside poles, and $\mathcal{U}_O$ be the union of Voronoi balls centered at outside poles. Let $U_I = \delta\mathcal{U}_I$ and $U_O = \delta\mathcal{U}_O$ be the boundaries of these unions.

Observation 1 *Every sample $s \in S$ lies on both U_I and U_O.*

4 Geometric accuracy

The result in this section is that the union boundaries U_I and U_O are both close to W under the assumption that S is a sufficiently dense sample. We formalize this assumption using the following definitions [1].

Definition: The *Local Feature Size* at a point $w \in W$, written $LFS(w)$, is the distance from w to the nearest point of the medial axis of W.

Definition: $S \subseteq W$ is an *r-sample* if the distance from any point $x \in W$ to its closest sample in S is at most a constant fraction r times $LFS(x)$.

For convenience, we define $r' = r/(1-r) =$

$O(r)$.

Assumption: We assume that S is a r-sample from W and $r \leq 0.1$.

One key idea is that under this assumption, the Voronoi cell of every sample $s \in S$ is long, skinny and roughly perpendicular to W. More precisely, given a sample s and a point v in its Voronoi region, the angle between the vector $\vec{sv}$ from s to v and the surface normal $\vec{n}$ at s has to be small (linear in r) when v is far away from s (as a function of LFS).

Lemma 2 (Amenta and Bern [1]) *Let s be a sample point from an r-sample S. Let v be any point in $Vor(s)$ such that $d(v,s) \geq \kappa LFS(s)$ for $\kappa > r'$. Let α be the angle between the vector $\vec{sv}$ and the surface normal $\vec{n}$ at s. Then $\alpha \leq \arcsin r'/\kappa + \arcsin r'$.*

Conversely, if the angle is large, then point v has to be close to s. Specifically, if $\alpha \geq \arcsin r'/\kappa + \arcsin r'$, then $d(v,s) \leq \kappa LFS(s)$. Rearranging things, we get:

Corollary 3 *For any v such that $\alpha \geq \arcsin r'$, we have $d(v,s) \leq \kappa LFS(s)$ with*

$$\kappa = \frac{r'}{\sin(\alpha - \arcsin r')}$$

Our first lemma says that inside balls can only intersect outside balls shallowly, if at all. We measure the depth of the intersection by the angle at which the balls intersect, as in Figure 3.

Lemma 4 *Let B_I be an inside Voronoi ball and B_O be an outside Voronoi ball. B_I and B_O intersect at an angle of at most $2\arcsin 3r = O(r)$.*

Proof: Consider the line segment connecting c_I and c_O, the centers of B_I and B_O. Since c_I and c_O lie on opposite sides of W, this segment crosses W in at least one point x.

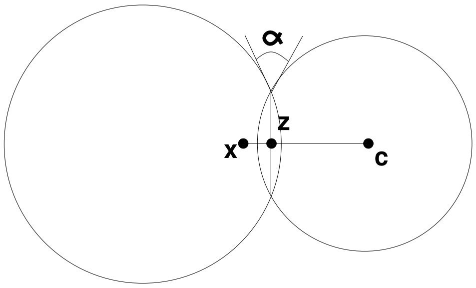

Figure 3: An inside and outside ball can intersect only at a small angle α.

Let $B(c,\rho)$ be the smaller of the two balls of radii of B_I and B_O. If $x \in B(c,\rho)$, we have $LFS(x) \leq 2\rho$. Since, the polar ball , $B(c,\rho)$ contains a point of the medial axis (Corollary **??**).

Otherwise x is in the larger of the two balls, but not in the smaller, as in Figure 3. Let c be the center of the smaller ball, let z be the center of the circle C in which the boundaries of B_I and B_O intersect, and let λ be the radius of C. By Corollary 7, we have $LFS(x) \leq d(x,c) + \rho = d(x,z) + d(z,c) + \rho$. But the distance from x to the nearest sample is at least

$$\sqrt{\lambda^2 + d^2(x,z)} = \sqrt{\rho^2 - d^2(z,c) + d^2(x,z)}$$

So the r-sampling requirement means that

$$\sqrt{\rho^2 - d^2(z,c) + d^2(x,z)} \leq r[\rho + d(x,z) + d(z,c)]$$

Since $d(z,c) \leq \rho$, we can simplify to

$$d(x,z) \leq 2r'\rho$$

which, for $r \leq 1/3$, means that x is very close to $B(c,\rho)$, and $LFS(x) \leq 3\rho$.

Since the distance from x to the nearest sample is at least λ and at most $3r\rho$, $\lambda \leq 3r\rho$. The angle between the plane P containing C and a tangent plane on $B(c,\rho)$ at C is thus at most $\arcsin 3r$, the angle between P and the tangent plane of the larger

ball is smaller, and the two balls meet at an angle of at most $2\arcsin 3r$.
□

A *medial ball* is a maximal ball with no points of W in its interior; the center of a medial ball is a point of the medial axis. The next lemma shows that a similar fact holds when one of the balls is a medial, rather than a polar, ball.

Lemma 5 *Let B_p be an inside (outside) polar ball and let B_m be an outside (inside) medial ball. The angle at which B_p and B_m intersect is at most $2\arcsin 2r = O(r)$.*

Proof: Similar to the previous lemma.
□

We can infer that the surface cannot penetrate too far into the interior of either union, as a function of the radii of the balls. But this does not yet give a bound in terms of LFS, which could be much smaller than the radius of either medial ball at a surface point x.

Lemma 6 *Let u be a point in the Voronoi cell of s but outside both polar balls at s. The distance from u to s is $O(r)LFS(s)$.*

Proof: We assume without loss of generality that $LFS(s) = 1$. Let p_1 be the pole farther from s. If $\angle usp_1 \leq \pi/2$, we let $p = p_1$, otherwise we consider $p = p_2$, the pole nearer to s. We let $B_{p,\rho}$ be the polar ball centered at p. In either case $d(u, s) \leq \rho$, because of the way in which the poles were chosen. Let θ be the angle between vectors $\vec{su}$ and $\vec{sp}$. Since u is outside the polar ball,

$$d(s, u) \geq 2\rho\cos\theta$$

Since $d(s, u) \leq \rho$, we have $\theta \geq \frac{\pi}{3} > 3\arcsin r'$. Let $\vec{n}$ represent the normal at s. We find $\angle\vec{n}\ \vec{sp} < 2\arcsin r'$ by Lemma 2. So $\angle\vec{n}\ \vec{su} > \pi/3 - 2\arcsin r' > \arcsin r'$. From Corollary 3 it follows that, for any point u in the Voronoi cell of s,

$$d(u, s) \leq \frac{r'}{(sin(\theta - 3\arcsin r'))}$$

Since $\theta \geq \frac{\pi}{3}$ the angle, $(\theta - 3\arcsin r') \geq \frac{\pi}{6}$. Which means that ,

$$d(u, s) \leq 2r'$$

Since we assumed $LFS(s) = 1$, the lemma follows.
□

The Voronoi cell of a sample $s \in W$ must contain the point of the medial axis induced by s. Since this point is atleast at a distance $LFS(s)$ from s, we get the following corollary.

Corollary 7 *Every polar ball contains a point of the medial axis.*

It remains to bound the distance from any point on the boundary of one union and in the interior of the other, to the surface.

Observation 8 *If d(u,s)= O(r)LFS(u) then d(u,s)=O(r)LFS(s) as well.*

Lemma 9 *For a point u on U_I (resp. U_O) and inside U_O (resp. U_I), the distance to the closest sample s is $O(r)LFS(s)$.*

Proof: Without loss of generality let u be a point on U_O and inside U_I. The line joining the centers of the balls B_O and B_I intersects the surface at some point x. Let s_x be the closest sample to x and let s be the closest sample to u. A ball centered at x, and with radius $d(s, s_x)$, should also contain u, as u to closer to x than s_x,which is outside both B_O and B_I. This and the r-sampling condition give a bound on $d(x, u)$.

$$d(x,u) \leq d(x,s_x) = O(r)LFS(x)$$

From the triangle inequality ,

$$d(u,s_x) \leq d(u,x) + d(x,s_x) = O(r)LFS(x) \tag{1}$$

Since s is the closest sample from u, we get

$$d(x,s) \leq d(x,u) + d(u,s) \leq d(x,u) + d(u,s_x)$$

Which gives, $d(x,s) = O(r)LFS(x)$. The LFS function is Lipshitz, that is $|LFS(p) - LFS(q)| \leq d(p,q)$. From equation 1 we then get

$$d(u,s) \leq d(u,s_x) = O(r)LFS(s)$$

□

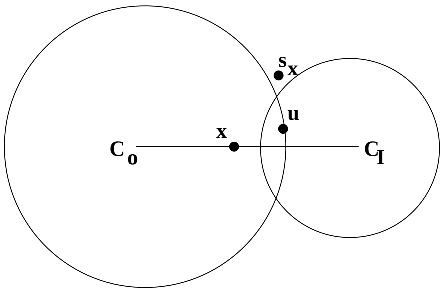

Figure 4: The point u is closer to x than s_x, which is outside both the balls.

Theorem 10 *The distance from a point $u \in U_I$ or $u \in U_O$ to its closest point on the surface $x \in W$ is $O(r)LFS(x)$.*

Proof: The point x is at least as close to u as s, and hence is within $O(r)LFS(s)$ of s. Since $|LFS(x) - LFS(s)| \leq d(x,s)$, the result follows from Lemma 6 and Lemma 9. □

This theorem tells us that most of $\mathbb{R}^3$ is contained in exactly one of the two unions of balls. A small part - the region within $O(r)LFS$ of W - is contained in both, or neither.

Now we show that the normals on U_I and U_O are also close to the normals of nearby points of W, approaching the correct normal as $O(\sqrt{r})$ as $r \rightarrow 0$.

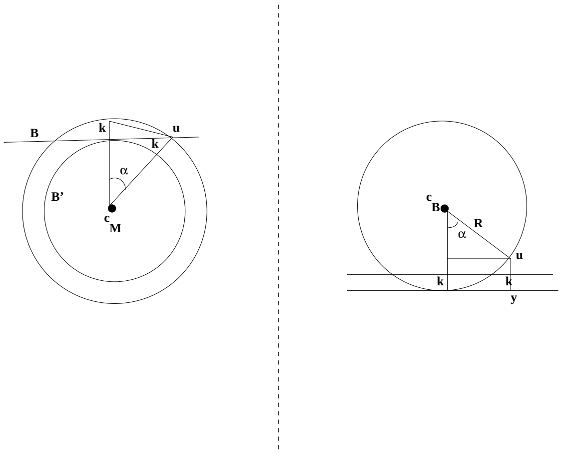

Figure 5: Since B cannot intersect B_M very deeply, and $d(u,x)$ has to be small, the indicated angle cannot be too large.

Observation 11 *Let $B_{c,\rho}$ be a polar ball, at distance at most k from a point $x \in W$. Then $\rho \geq \frac{LFS(x)-k}{2}$.*

This follows because B is a polar ball, so it contains a point of the medial axis, by Corollary 7, while the nearest point of the medial axis to x is at distance $LFS(x)$.

Lemma 12 *Let u be a point such that the distance to the nearest point $x \in W$ is at most $O(r)LFS(x)$. Let $B = B_{c,\rho}$ be a polar ball containing u. Then the angle, in radians, between the surface normal at x and the vector $\vec{uc}$ is $O(\sqrt{r})$.*

Proof: The angle we are interested in is $\alpha = \angle uc_Bc_M + \angle uc_Mc_B$. We begin by bounding $\angle uc_Mc_B$. Without loss of generality, assume $LFS(x) = 1$.

Since B_M is the medial ball at x, the radius R of B_M is at least one. Since B

and B_M cannot intersect at x at an angle greater than $2\arcsin 2r$ (Lemma 5), the thickness of the lune in which they intersect is at most a factor of $O(r^2)$ times the smaller of the two radii. So we can assume B is tangent to a ball B' of radius $R(1-O(r^2))$, concenteric with B_M. Let $k = d(u, B') = O(r^2)R + O(r)$, as on the left in Figure 5, where the angle we are bounding is α. If $R > 1$, then k is a smaller fraction of R, and $\angle uc_Mc_B$ will be smaller, so we assume in the worst case that $R = 1$. Increasing the radius ρ of B, on the other hand, increases the angle so we assume that B is infinitely large. Angle $\angle uc_Mc_B$, then, is $O(\sqrt{k/R}) = O(\sqrt{r})$.

We use a similar argument to bound $\angle uc_Bc_M$. Note that by Observation 11, the radius ρ of B is at least $(1 - d(u,x))/2$. Again the worst case occurs when $\rho = \Omega(1)$ and B_M is infinitely large. In that case B is tangent to another infinitely large ball, offset from B_M by a distance of $O(r^2)\rho$. Extending segment ux to hit this ball, as on the right in Figure 5, gives us a point y at distance $k = O(r^2)\rho + O(r)$ from u, and we find $\angle uc_Bc_M = O(\sqrt{k/\rho}) = O(\sqrt{r})$.
□

5 Homeomorphism

We use these geometric theorems to show that the surface of either U_I or U_O is homeomorphic to the actual surface W. We'll do this using a natural map from U to W.

Definition: Let $\mu : R^3 \to W$ map each point $q \in R^3$ to the closest point of W.

Lemma 13 *Let U be either U_I or U_O. The restriction of μ to U defines a homeomorphism from U to W.*

Proof: We consider U_I; the argument for U_O is identical. Since U_I and W are both compact, it suffices to show that μ defines a continuous, one-to-one and onto function. The discontinuities of μ are the points of the medial axis. From Theorem 10, every point of U_I is within distance $O(r)LFS(x)$ from some point $x \in W$, wheras every point of the medial axis is at least $LFS(x)$ from the nearest point $x \in W$. Thus μ is continuous on U_I.

Now we show that μ is one-to-one. For any $u' \in U_I$, let $x = \mu(u')$ and let $n(x)$ be the normal to W at x. Orient the line $l(x)$ through x with direction $n(x)$ according to the orientation of W at x. Any point on U_I such that $\mu(u) = x$ must lie on $l(x)$; let u be the outer-most such point.

Let $B_{c,\rho}$ be the ball in U_I with u on its boundary. Let α be the angle between $\vec{uc}$ and the surface normal $n(x)$. We have $d(u,x) = O(r)LFS(x)$ from Lemma 10, so that $\alpha = O(\sqrt{r})$, by Observation 12. Meanwhile $\rho = \Omega(LFS(x))$, by Observation 11.

Point u' is at most $O(rLFS(x))$ from u, while $l(x)$ lies in the interior of B for distance at least $2\rho\cos\alpha = O(LFS(x))$. Since u' must be on $l(x)$ but outside of B, and u is the outermost such point, it must be the case that $u = u'$.

Finally, we need to establish that $\mu(U)$ is onto W. Since μ maps U, a closed and bounded surface, continuously onto W, $\mu(U)$ must consist of some subset of the closed, bounded connected components of W. But since every connected component of W contains samples of S, and $\mu(s) = s$ for $s \in S$, $\mu(U)$ must consist of all the connected components of W.
□

6 Medial axis approximation

Edelsbrunner defined the *dual shape* of a union of balls as the weighted α-shape defined by the balls, at $\alpha = 0$. Let D_I and D_O be the dual shapes of $\mathcal{U}_I$ and $\mathcal{U}_O$, respecively. He showed that the dual shape is *homotopy equivalent* to the union itself, by giving a continuous *deformation retraction* of the union onto the dual shape. This is a way of saying that the union and its dual shape have the same holes, tunnels and connected components, even where they differ in dimension. Similarly, a shape and its medial axis are homotopy equivalent (a very similar deformation retraction, in fact, is given in [4]). Let M_I and M_O be the medial axes of the unions $\mathcal{U}_I$ and $\mathcal{U}_O$, respectively.

Theorem 14 *Both D_I and M_I are homotopy equivalent to $\mathcal{W}$, and both D_O and M_O are homotopy equivalent to $\mathbb{R}^3 - \mathcal{W}$.*

Proof Sketch: The functions $\mu : U_I \rightarrow W$ and $\mu : U_O \rightarrow W$ can be extended to space homeomorphisms taking $\mathcal{U}_I$ to $\mathcal{W}$ and $\mathcal{U}_O$ to $\mathbb{R}^3 - \mathcal{W}$, respectively.
□

In addition to this topological equivalence,

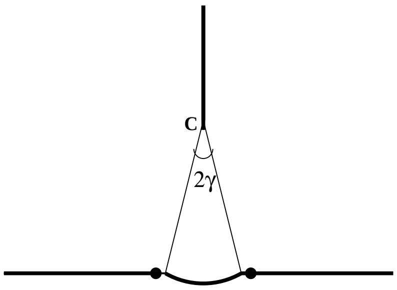

Figure 6: A small bump on the surface induces a long "hair" on the medial axis without having to contain any samples. Here, c is the endpoint of the "hair", and r is about $1/2$, so that neither of the samples lies on the bump.

we show that the set P_I of interior poles converges, geometrically, to the true medial axis of $\mathcal{W}$ the sampling density increases (a similar fact holds for P_O). In contrast to our previous results, we cannot guarantee that every medial axis is adequately approximated by an r-sample for a specific value of r such as 0.1. This is because, as in Figure 6, for any finite value of r, we can construct a a very small, shallow bump on the surface W, inducing a "hair" on the medial axis but without requiring samples on the bump. Note, however, that the angle γ has to be very small. This motivates the following definition.

Definition: A medial axis point c belongs to the γ-medial axis of $\mathcal{W}$ when at least two points $u_1, u_2 \in W$ on the boundary of the medial ball centered at c form an angle $\angle u_1 c u_2 > 2\gamma$.

Interestingly, the γ-medial axis can be disconnected.

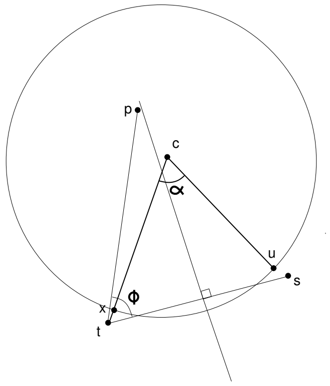

Figure 7: Since p is in the Voronoi cell of t, it has to be on the same side of the bisector of ts as t.

Lemma 15 *Let $B_{c,\rho}$ be a medial ball such that c belongs to the γ-medial axis, for some fixed γ. Then the pole of the nearest sample converges to c, as $r \rightarrow 0$.*

Proof: Let t be the closest sample to c. Let α be the maximum of of angles $\angle tcu_1$ and $\angle tcu_2$, and let $u \in \{u_1, u_2\}$ be the one realizing the maximum. Then $\alpha \geq \gamma$. Let s be u's closest sample.

From the sampling criterion we have that $d(u, s) \leq rLFS(s) \leq r\rho$. Let x be the point at which segment ct intersects the medial ball. Since $\angle xcu = \alpha$, $d(t,u) \leq 2\rho \sin\alpha$. Also, $d(c,t) \leq d(c,s) \leq \rho(1+r)$, so $d(x,t) \leq r\rho$. We conclude that $d(t,s) \leq 2\rho(r + \sin\alpha)$.

In the Voronoi cell of t, $d(c,t) \geq LFS(t)$. So from Lemma 2, both $\angle\vec{n}\vec{tc}$ and $\angle\vec{n}\vec{tp}$ are at most $2\arcsin r'$, where $\vec{n}$ is the surface normal at t. So $\angle ctp \leq 4\arcsin r' = \beta$.

From Figure 7, some tedious calculations show that $\angle uts < \arcsin(\frac{r}{2\sin(\frac{\alpha}{2})}) = \epsilon$. So we can bound the angle $\phi = \angle pts$, as $\phi \leq \frac{\pi}{2} - \frac{\alpha}{2} + \beta + \epsilon$.

Since c is point in the Voronoi cell of t

$$\rho \leq d(t,c) \leq d(t,p)$$

Since p is t's pole, it lies on the same side of the bisector of ts as t. So we can bound $d(t,p)$:

$$d(t,p) \leq \frac{\rho(r + \sin\frac{\alpha}{2})}{\sin(\frac{\alpha}{2} - \beta - \epsilon)}$$

We choose $\alpha = \omega(r)$, for example $\sqrt{r}$. Then as r goes to zero, the expression on the right approaches ρ, since β and ϵ are both $O(r)$. The angle $\angle ptc$ goes to zero as well, so p converges to c.
$\square$

Since $\gamma \to 0$ as $r \to 0$, we get the following:

Theorem 16 *The set of interior poles converges to the interior medial axis of $\mathcal{W}$ as $r \to 0$.*

Proof: The Voronoi cell of any sample s contains the interior medial axis point c corresponding to s. There is some value of γ_0 small enough so that c belongs to the γ-medial axis for $\gamma \leq \gamma_0$. So there is some r_0 small enough so that by Lemma 15, the interior pole of s converges to c. Similarly, any medial axis point c lies in the Voronoi cell of some sample s (which might change as r decreses). Again, there is some r_0 small enough so that the distance from the interior pole of s to c converges to zero.
$\square$

7 Discussion

As we observed in the introduction, the set P_I of inner poles is generally much smaller than the entire set P_V of inner Voronoi vertices. Yet we proved that the union of the inner poles gives a good geometric and topological approximation of shape when the sample S is sufficiently dense. Quite possibly one could prove that the boundary U_V of the union of all inner Voronoi balls is also close to, and homeomorphic to, the actual object surface, under a similar sampling assumption, but the surface normals on U_V can differ significantly from the correct normals, even for arbitrarily dense samples.

We showed that the set of poles converges to the true medial axis as the sampling density increases. A good next step would be to show that both the medial axis of $\mathcal{U}_I$ and the dual shape of $\mathcal{U}_I$ converge to the true medial axis as well.

Applications using the union of balls representation usually require simplifying the model for practical reasons. We believe that a simplification process with provable bounds on the error introduced should be possible given the bounds we have on the quality of U_I.

8 Acknowlegments

We gratefully acknowlege Marshall Bern for helpful discussions on medial axis approximation. We thank Sunghee Choi for producing some of the models, and for her helpful discussions in the early stages of this project. We thank Justin Lee for producing the images of unions of balls. We are very grateful for the high-quality free software we used to make the images: Ken Clarkson's `hull`, Jonathan Shewchuk's exact determinant functions, and the raytracer `POVray`.

References

[1] N. Amenta and M. Bern. Surface reconstruction by Voronoi filtering. *Discrete and Computational Geometry* **22**, pp. 481–504, (1999).

[2] D. Attali and A. Montanvert. Computing and Simplifying 2D and 3D Continuous Skeletons, *Computer Vision and Image Understanding*, 67(3) (1997), pp. 261–273.

[3] S-W. Cheng, H. Edelsbrunner, P. Fu, and K-P. Lam. Design and analysis of planar shape deformation *Proceedings of the 14th Annual ACM Symposium on Computational Geometry* pp. 29–38, (1998).

[4] H.I. Choi, S.W. Choi and H.P. Moon. Mathematical theory of medial axis transform, *Pacific Journal of Mathematics* 181(1), pp. 57–88, (1997).

[5] T. Culver, J. Keyser, and D. Manocha. Accurate computation of the medial axis of a polyhedron, UNC Technical Report TR98-038. Appeared in *Proc. ACM Solid Modeling*, 1999.

[6] H. Edelsbrunner. The union of balls and its dual shape, *Proceedings of the 9th Annual ACM Symposium on Computational Geometry*, pp, 218-231, (1993).

[7] J. Goldak, X. Yu, A. Knight, and L. Dong. Constructing discrete medial axis of 3-D objects. *Int. J. Computational Geometry and its Applications* 1 (1991) 327–339.

[8] P. Hubbard. Approximating polyhedra with spheres for time-critical collision detection, *ACM Transactions on Graphics*, 15(3), pp. 179–210, (1996).

[9] V. Ranjan and A. Fournier. Matching and Interpolation of Shapes using Unions of Circles, *Computer Graphics Forum*, 15(3), pp. 129–142, (1996).

[10] D. Sheehy, C. Armstrong and D. Robinson. Shape description by medial axis construction, *IEEE Transactions on Visualzation and Computer Graphics*, 2(1), pp. 62–72, (1996).

[11] M. Teichman and S. Teller. Assisted Articulation of Closed Polygonal Models, *Proc. 9th Eurographics Workshop on Animation and Simulation*, (1998).